

# Thermal stability and mechanical properties of a Zr-based bulk amorphous alloy

D. Fátay<sup>a</sup>, J. Gubicza<sup>a,b,\*</sup>, P. Szommer<sup>a</sup>, J. Lendvai<sup>a</sup>, M. Blétry<sup>c</sup>, P. Guyot<sup>c</sup>

<sup>a</sup> Department of General Physics, Eötvös University, Pázmány Péter Sétány 1/A, H-1117 Budapest, Hungary

<sup>b</sup> Department of Solid State Physics, Eötvös University, Budapest, Hungary

<sup>c</sup> LTPCM, Institut National Polytechnique de Grenoble, France

Received 19 September 2003; received in revised form 20 January 2004

## Abstract

The thermal and mechanical properties of a Zr–Al–Cu–Ti–Ni bulk metallic glass were investigated. The glass transition and the crystallization were studied by calorimetry and X-ray diffraction. It was found that the crystallization occurred in two steps. The precipitating phases, and the activation energies were determined. It was established that the crystallization was controlled by the diffusion of the alloying Cu and Ni atoms. The creep behavior was investigated by indentation tests. The viscosity and the activation energy of the deformation process determined from indentation were in reasonable agreement with those obtained by compression tests.

© 2004 Elsevier B.V. All rights reserved.

**Keywords:** Bulk metallic glass; Calorimetry; X-ray diffraction; Indentation creep test

## 1. Introduction

Before 1990 the production of metallic glasses required high cooling rates ( $>10^5$  K/s) to prevent crystallization of the alloy [1,2]. As a result, amorphous alloys were solidified in the form of very thin ribbons or wires. This shape of metallic glasses makes the mechanical testing difficult and restricts the engineering applicability of the material. New processing techniques and new multicomponent materials enabled the decrease of the critical cooling rate well below 10 K/s [2,3]. The low cooling rate results in production of amorphous alloys in bulk form.

Bulk metallic glasses have unique mechanical properties including high strength and low Young's modulus, moreover good forming ability in the vicinity of the glass transition temperature [4–6]. In this temperature regime the stability of the amorphous structure and the creep behavior are important factors in engineering applications.

In this paper the thermal and creep properties of a Zr-based bulk metallic glass are studied. The glass transition and the crystallization are investigated by differential scanning calorimetry (DSC) and X-ray diffraction. The

creep behavior in the vicinity of the glass transition temperature is studied by indentation creep tests. The indentation technique is an effective tool for studying creep properties of bulk metallic glasses because there is no need for special sample preparation and a small amount of sample is enough for testing [7]. Results obtained from indentation are compared with those determined by compression tests.

## 2. Experimental details

Bulk metallic glass samples with the composition of Zr–10 at.% Al–27 at.% Cu–2.5 at.% Ti–8 at.% Ni were prepared by the copper mold technique [8]. The diameter and the length of the cylindrical specimens were 5 and 50 mm.

The thermal behavior of the alloy was studied by conventional differential scanning calorimetry (DSC) and by temperature modulated DSC (TMDSC) measurements. The heating rate in the DSC measurements varied between 4 and 32 K/min. In the TMDSC measurements the heating rate was 1 K/min which was modulated by a sine temperature oscillation with 1 K amplitude and at 0.01 Hz frequency.

The crystalline phases were identified by X-ray diffraction. The X-ray diffractograms were measured by a Philips Xpert powder diffractometer (Bragg–Brentano geometry)

\* Corresponding author. Tel.: +36-1-372-2876; fax: +36-1-372-2811.  
E-mail address: gubicza@ludens.elte.hu (J. Gubicza).

with Cu K $\alpha$  radiation ( $\lambda = 0.15418$  nm). The grain size of the crystalline phases was determined from the full width at half maximum (FWHM) using the Scherrer equation [9].

The creep behavior was studied by indentation test using a Setaram TMA-92 thermomechanical analyzer between the temperatures of 715 and 725 K. The indentation measurements were carried out by using a cylindrical punch of 1.2 mm in diameter under constant load which can be varied between 0.5 and 1.5 N. The pressure calculated from the load was between 0.4 and 1.4 MPa. At lower temperatures (675–687 K) where higher pressure is required for a considerable creep deformation, an indentation creep device [7] was used with a cylindrical indenter of 1.5 mm in diameter. In this case the applied load was varied between 100 and 180 N which corresponds to a pressure between 56 and 102 MPa.

### 3. Results and discussion

Fig. 1 shows a DSC curve recorded at 8 K/min heating rate. The glass transition temperatures at 8 K/min heating rate were found to be  $T_{g1} = 677 \pm 2$  K and  $T_{g2} = 693 \pm 3$  K.  $T_{g1}$  was determined as the temperature where the DSC curve deviates from the baseline at the beginning of the endothermic effect.  $T_{g2}$  is the temperature at the inflection point of the DSC curve during the glass transition.

The change of the specific-heat ( $\Delta c_p$ ) in glass state was calculated as a function of temperature by derivating the heat flow–temperature curve obtained from the TMDSC measurements. The glass transition temperatures were obtained to be  $T_{g1} = 670 \pm 3$  K and  $T_{g2} = 697 \pm 3$  K. The temperature  $T_{g1}$  was determined as the value where the curve of the  $\Delta c_p$  deviates from the straight line fitted to the initial part of the curve, and  $T_{g2}$  was obtained as the temperature at the inflection point of the  $\Delta c_p$  curve (Fig. 2). The slight dif-

ference between the glass transition temperatures obtained from DSC and TMDSC measurements can be understood from the different heating rates applied in the two methods.

In the DSC curve of Fig. 1 the two exothermic peaks at 754 ( $T_{x1}$ ) and 852 K ( $T_{x2}$ ) correspond to two crystallization steps. The heats released during the first and the second crystallization steps were 55.4 and 12.5 J/g, respectively. The temperature of the onset of crystallization,  $T_{xo}$  (determined as the intercept of the rising edge and the calorimetric baseline) was  $752 \pm 2$  K. The glass forming ability is characterized by the difference between  $T_{xo}$  and  $T_{g1}$  determined from the DSC curve:  $\Delta T_{xg} = 75$  K. If the crystallization is supposed to be controlled by thermally activated processes, the activation energy can be determined from the shifting of the  $T_x$  peak temperatures with varying heating rate ( $\beta$ ) of the linear heating DSC scans on the basis of the Kissinger-equation [10]:

$$\frac{\beta}{T_x^2} = \frac{ZR_g}{Q_x} \exp\left(-\frac{Q_x}{R_g T_x}\right), \quad (1)$$

where  $R_g$  is the gas constant,  $Z$  is the frequency factor and  $Q_x$  is the activation energy. The activation energies for the first and second crystallization peaks obtained from the Kissinger-plots are  $Q_{x1} = 243 \pm 24$  kJ/mol and  $Q_{x2} = 274 \pm 13$  kJ/mol, respectively.

Fig. 3 shows the X-ray diffractograms obtained in the as-cast state and after heating at 8 K/min heating rate up to 800 K (beyond the first crystallization peak) and 905 K (beyond the second crystallization peak). The as-received specimen is fully amorphous. After the first crystallization step mainly the metastable fcc  $Zr_2Ni$  phase ( $Ti_2Ni$  type) precipitated with the lattice parameter of 1.205 nm which is smaller than 1.227 nm reported in [11]. This phase is stabilized by the oxygen atoms accommodated in the unit cell in addition to the 96 metal atoms. The  $Zr_2Ni$  phase reported in [11] contains 4.1 at.% oxygen. The lower lattice parameter

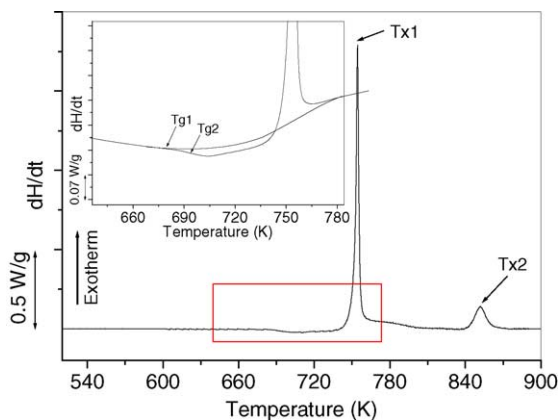


Fig. 1. DSC curve measured at 8 K/min heating rate. The inset shows the DSC curve in the vicinity of the glass transition in higher magnification. The glass transition temperatures,  $T_{g1}$  and  $T_{g2}$  were determined as the temperature where the DSC curve deviates from the baseline and from the inflection point of the curve, respectively.

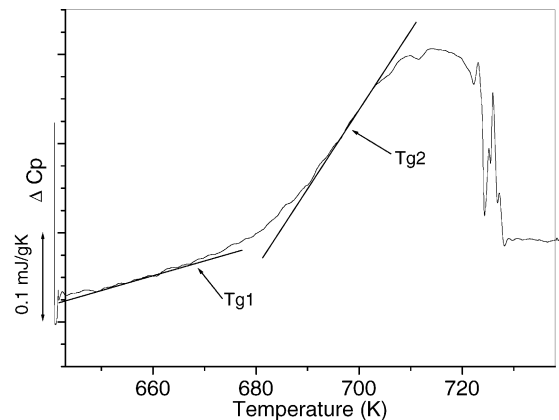


Fig. 2. Change of the specific-heat ( $\Delta c_p$ ) as a function of temperature obtained from TMDSC measurement at 1 K/min heating rate.  $T_{g1}$  was determined as the temperature where the curve deviates from the straight line fitted to the initial part of the curve and  $T_{g2}$  is the temperature at the inflection point of the curve.

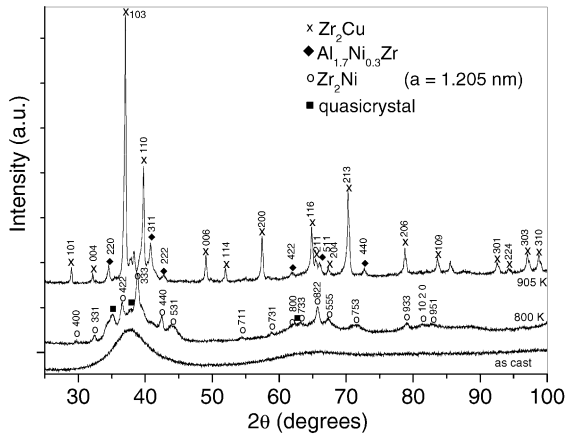


Fig. 3. X-ray diffraction patterns of the as-cast specimen and of samples heated in the DSC up to 800 and 905 K, respectively.

of  $Zr_2Ni$  phase determined in the present work can be related to a lower oxygen content. The average grain size of the  $Zr_2Ni$  phase was  $41 \pm 4$  nm. A quasicrystalline phase and residual amorphous material were also detected in the diffractogram. The quasicrystalline phase was identified on the basis of diffractograms presented in [12,13]. After the second crystallization step, mainly tetragonal  $Zr_2Cu$  (Powder Diffraction File, PDF number: 18-0466) was formed with  $18 \pm 2$  nm average grain size, however, traces of the cubic  $Al_{1.7}Ni_{0.3}Zr$  phase (Cu<sub>2</sub>Mg type, PDF number: 20-0036) were also detected. In  $Zr_2Cu$  phase the substitution of Cu by Ni or Al could occur, therefore  $Zr_2Cu(Ni,Al)$  would be the appropriate notation for this phase [14,15].

The activation energies of the first and second crystallization steps determined in this paper (243 and 274 kJ/mol, respectively) and the activation energy of Ni diffusion in a bulk amorphous Zr–8.25 at.% Ti–7.5 at.% Cu–10 at.% Ni–27.5 at.% Be alloy presented in [16] (266 kJ/mol) are close to each other. Since Cu and Ni are neighboring elements in the periodic table and they have similar atomic radius, it seems to be logical to assume that the diffusion activation energy of Cu in Zr-based amorphous alloys is close to that of Ni diffusion. The relatively good agreement between the crystallization activation energies and the activation energy for Ni or Cu diffusion is probably due to the fact that the crystallization of the  $Zr_2Ni$  or  $Zr_2Cu(Ni,Al)$  main phases requires long-range diffusion of Ni and Cu atoms. It has to be noted, however, that beside the diffusion energy there are further factors influencing the activation energy of crystallization (e.g. surface energy).

The temperature dependence of the mechanical behavior of the as-cast specimen was investigated by increasing the temperature at 8 K/min heating rate under constant pressure (102 MPa) in the indentation creep machine (Fig. 4). For comparison the DSC curve obtained on the as-cast sample at 8 K/min heating rate is also shown in the figure. The indentation rate of the amorphous alloy increases rapidly with the temperature between  $T_{g1}$  and  $T_{x1}$  as a result of

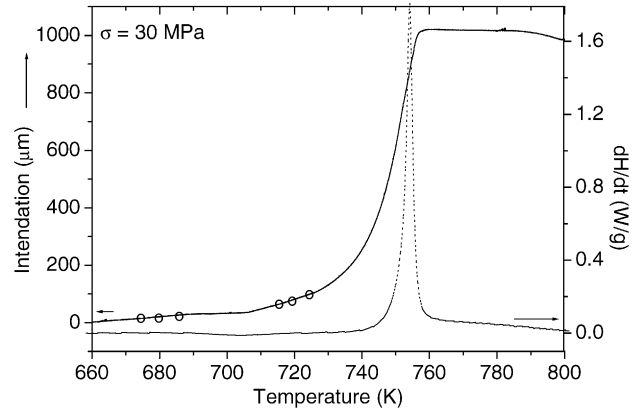


Fig. 4. Indentation depth–temperature curve obtained at constant pressure of 102 MPa and heating rate of 8 K/min (solid line) and the corresponding DSC curve (dotted line). The temperatures of the isothermal indentation creep tests are indicated by open circles on the indentation curve.

decreasing viscosity. The indentation stops when more than 90% of the crystallization is completed (see the DSC curve in Fig. 4). Isothermal indentation creep tests were carried out at the six temperatures indicated by open circles on the indentation curve of Fig. 4 (at 675, 680, 687, 715, 720 and 725 K). These temperatures were selected to be well below the onset crystallization temperature (752 K) to avoid the effect of crystalline phases on creep behavior. From the steady state stage of the creep curves the viscosity ( $\eta$ ) was determined using the following equation:

$$\eta = \frac{\sigma}{3\dot{\epsilon}}, \quad (2)$$

where  $\sigma$  is the stress and  $\dot{\epsilon}$  is the strain rate. It is generally assumed that the equivalent stress and strain rate in indentation creep tests can be expressed by the applied pressure ( $p$ ) and the indentation rate ( $\dot{h}$ ), respectively [7]:

$$\sigma = \frac{p}{3} \quad (3)$$

and

$$\dot{\epsilon} = \frac{\dot{h}}{d}, \quad (4)$$

where  $d$  is the diameter of the cylindrical indenter.

The viscosity did not change when the stress was changed at constant temperature, which means that the alloy behaved as a Newtonian liquid near the glass transition temperature. The viscosity decreased from  $2 \times 10^{12}$  Pa s to  $2 \times 10^9$  Pa s when the temperature was raised from 675 to 725 K. The activation energy characterizing the deformation process was determined from the  $\ln(\eta) - 1/T$  plot as  $563 \pm 16$  kJ/mol (Fig. 5). The creep properties of a bulk metallic glass of the same composition were investigated recently by compression tests [17]. The temperature range was narrower (between 683 and 703 K) than in the present indentation experiments. At low strain rate values the material was found to deform by Newtonian flow while above a critical strain rate a non-Newtonian behavior was observed.

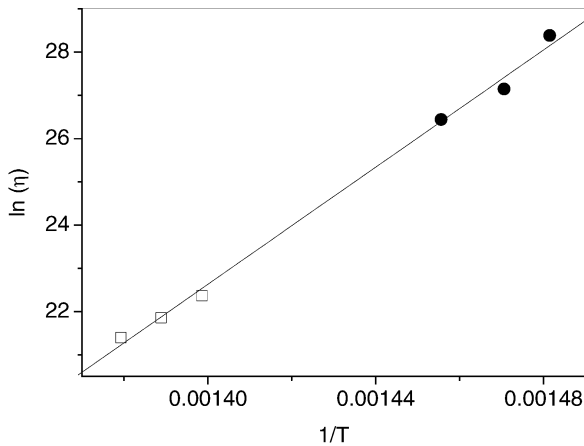


Fig. 5.  $\ln(\eta) - 1/T$  plot. The viscosity values obtained by indentation creep tests and by TMA are represented by solid circles and open squares, respectively.

The critical strain rate increases with increasing the temperature. Between 683 and 703 K the critical strain rate is about  $10^{-3}$  to  $10^{-4} \text{ s}^{-1}$ . Leonhard et al. [18] have also found for Zr–30 at.% Cu–10 at.% Al–5 at.% Ni bulk amorphous alloy that between 683 and 702 K and below the strain rate of  $10^{-4} \text{ s}^{-1}$  the material behaved as a Newtonian liquid. Since in the present indentation creep tests the strain rate was in the order of  $10^{-5} \text{ s}^{-1}$  Newtonian creep behavior was expected. Although the stress applied in the compression tests (300 MPa) is by about an order of magnitude higher than that used in the indentation tests (34 MPa), the activation energy obtained from indentation (563 kJ/mol) is in reasonable agreement with the value (539 kJ/mol) determined by compression tests.

#### 4. Conclusions

The thermal and mechanical properties of a Zr–Al–Cu–Ti–Ni bulk metallic glass were investigated. The crystallization was found to occur in two steps. In the first crystallization step mainly metastable  $\text{Zr}_2\text{Ni}$ , while during the second step  $\text{Zr}_2\text{Cu}(\text{Ni},\text{Al})$  phase was formed. Indentation tests were applied to investigate the creep properties at lower stress and

strain rate as well as in a wider temperature range than it has been done by compression tests in another study [17]. The indentation creep tests showed that near the glass transition temperature (around 700 K) and at low strain rates (around  $10^{-5} \text{ s}^{-1}$ ) the material behaves as a Newtonian liquid. The activation energy of deformation (563 kJ/mol) determined in indentation is in reasonable agreement with that obtained by compression tests at higher stress and strain rate values.

#### Acknowledgements

This work was supported by the Hungarian Scientific Research Fund, OTKA, Grant Nos. T-043247 and F-047057 and by the F-17/00 Balaton project.

#### References

- [1] W. Klement, R.H. Willens, P. Duwez, *Nature* 187 (1960) 869.
- [2] A. Inoue, *Acta Mater.* 48 (2000) 279.
- [3] A. Inoue, N. Nishiyama, *Mater. Sci. Eng. A* 226–228 (1997) 401.
- [4] C. Gilbert, R.O. Ritchie, W.L. Johnson, *Appl. Phys. Lett.* 71 (1997) 476.
- [5] C.C. Hays, C.P. Kim, W.L. Johnson, *Phys. Rev. Lett.* 84 (2000) 2901.
- [6] A. Leonhard, L.Q. Xing, M. Heilmaier, A. Gebert, J. Eckert, L. Schultz, *Nanostruct. Mater.* 10 (1998) 805.
- [7] G. Cseh, N.Q. Chinh, P. Tasnádi, A. Juhász, *J. Mater. Sci.* 32 (1997) 5107.
- [8] Z.H. Gan, H.Y. Yi, J. Pu, J.F. Wang, J.Z. Xiao, *Scripta Mater.* 48 (2003) 1543.
- [9] A. Guinier, *X-ray Diffraction*, Freeman, San Francisco, 1963.
- [10] M.E. Kissinger, *Anal. Chem.* 29 (1957) 1702.
- [11] Z. Altounian, E. Batalla, J.O. Stromolsen, J.L. Walter, *J. Appl. Phys.* 61 (1987) 149.
- [12] B.S. Murty, D.H. Ping, K. Hono, A. Inoue, *Acta Mater.* 48 (2000) 3985.
- [13] N. Ismail, A. Gebert, M. Uhlemann, J. Eckert, L. Schultz, *J. Alloys Comp.* 314 (2001) 170.
- [14] A. Inoue, D. Kawase, A.P. Tsai, T. Zhang, T. Masumoto, *Mater. Sci. Eng. A* 178 (1994) 255.
- [15] J. Eckert, N. Mattern, M. Zinkevitch, M. Seidel, *Mater. Trans. JIM* 39 (1998) 623.
- [16] K. Knorr, M.-P. Macht, K. Freitag, H. Mehrer, *J. Non-Cryst. Solids* 250/252 (1998) 669.
- [17] M. Blety, P. Guyot, Y. Brechet, J.J. Blandin, J.L. Soubeyroux, this volume.
- [18] A. Leonhard, M. Heilmaier, J. Eckert, *Scripta Mater.* 43 (2000) 459.